MOLYBDENUM VALENCE IN BASALTIC SILICATE MELTS: EFFECTS OF TEMPERATURE AND PRESSURE. L. R. Danielson[1], K. Righter[2], M. Newville[3], S. Sutton[3,4], Y. Choi[3], K. Pando[1], [1]ESCG, Houston, TX 77058 United States (lisa.r.danielson@nasa.gov), [2]NASA JSC, 2101 NASA Parkway, Houston, TX 77058 United States, [3]Center for Advanced Radiation Sources and [4]Dept. of Geophys. Sci., University of Chicago, Chicago, IL 60637 United States.

Introduction: The metal-silicate partitioning behavior of molybdenum has been used as a test for equilibrium core formation hypotheses [for example, 1-6]. However, current models that apply experimental data to equilibrium core-mantle differentiation infer the oxidation state of molybdenum from solubility data or from multivariable coefficients from metal-silicate partitioning data [1,3,7].

Molybdenum, a multi-valent element with a valence transition near the fO_2 of interest for core formation (~IW-2) will be sensitive to changes in fO_2 of the system and silicate melt structure. In a silicate melt, Mo can occur in either 4+ or 6+ valence state, and Mo^{6+} can be either octahedrally or tetrahedrally coordinated. Here we present X-ray absorption near edge structure (XANES) measurements of Mo valence in basaltic run products at a range of P, T, and fO_2 and further quantify the valence transition of Mo.

Experiments: Compositions analyzed thus far include basalt, hawaiite, and ankaramite [8]. New experiments were conducted with Knippa basalt used as a starting material [as in 5]. The range of fO_2 was extended down to ΔIW-5. Temperatures and pressures from 1190 to 2200 ºC and 1 bar to 24GPa were investigated. Experiments at 10 kbar were conducted in piston cylinder apparatus; experiments at 16 GPa and 24 GPa were conducted utilizing multi-anvil techniques. Run charges were contained in graphite capsules.

For experiments conducted at 1bar, fO_2 was controlled by $CO-CO_2$ gas mixture. At pressures greater than 1 bar, Si metal was added to the starting composition to buffer fO2 according to Si + O2 = SiO2, following the technique of Berthet et al. [9], in order to extend the reducing conditions well below IW. Experiments above 1 bar pressures were conducted as metal-silicate partitioning runs, with 29% Fe by weight added to the basalt starting material [5]. Mo was added to these experiments at 1wt% level as MoO_3 [5], resulting in ppm levels of Mo in silicate.

Analyses: A monochromatic X-ray beam from a Si(111) double crystal monochromator was focused onto the sample and the fluorescent X-ray yield was plotted as a function of incident X-ray energy (more detail can be found in [9,10,11]). Mo K XANES spectra were normalized to strontium as an internal reference element, then normalized so that the below edge intensity was zero and the above edge intensity was unity. The oxidation state of molybdenum was then inferred from the energy of the K-edge position defined as the lowest energy where μ=1 in the normalized XANES spectrum [after 10,11]. Energy shift and intensity of the pre-edge peak was used to determine coordination of Mo^{6+} [10,12]. Mo foil, MoO_3 powder, MoO_2 powder, and experiment KR-D, the extreme oxidized end member Mo doped andesite were used as standards to form a linear trend for valence determination.

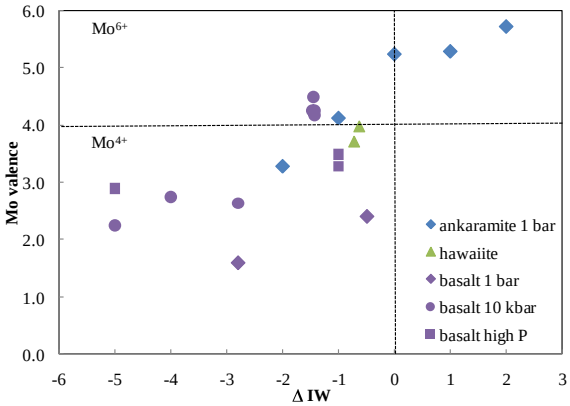

Figure 1. Molybdenum average valence as a function of oxygen fugacity relative to the iron-wüstite buffer for experiments in table 1. Highest pressure experiments are 16 and 24GPa.

Results and Discussion: Previous results [8], show a trend in ankaramite 1 bar experiments from an average valence of Mo^{6+} at the most oxidizing condition (IW+2) to nearly Mo^{3+} at IW-2 (Figure 1). The transition from Mo^{6+} to Mo^{4+} occurs largely between IW and IW-1, in good agreement with Holzheid et al. [1] and O'Neill and Eggins [7], who concluded Mo changed dominant valence at around IW-1, from Mo^{6+} to Mo^{4+}. Although O'Neill and Eggins [7] suggested that below IW, down to IW-3, Mo^{4+} and Mo^{6+} coexist in equal amounts, our results show Mo^{4+-6+} coexistence only occurs above IW-1. Below IW-1, Mo occurs as Mo^{4+}, with significant contribution of Mo of lower valence beginning at IW-2. At the conditions of core formation, near IW-2, Mo^{6+} is no longer present, and the average valence falls below Mo^{4+}. Knippa basalt 1 bar experiments are almost 2 valence units below those

for ankaramite at similar fO_2, which could be related to the higher FeO content of the Knippa basalt (14wt% compared to 17wt%).

Farges et al. [12] suggested the transition to Mo^0 dominance happens at around IW-3, with Mo metal precipitating at IW-4. This transition is consistent with the valence results of the Knippa basalt experiments at 1bar. However, high pressure experiments are generally a constant valence of ~$Mo^{+2.5}$ from IW-3 to IW-5. Unfortuneately, Farges et al. [13] find no evidence for the presence of Mo^{3+} nor Mo^{2+} in glasses, but also cannot rule out the possibility for contributions from these.

There is no systematic variation in pressure or temperature as a function of Mo valence. However, Knippa basalt experiments above 1 bar pressure seem to be generally one valence unit above experiments at 1 bar. This could also reflect the higher temperatures of these experiments relative to the 1 bar experiments. This is somewhat contradictory to Farges et al. [13], who found that from ambient temperature up to 1200 ºC and pressures of up to 7 kbar, Mo valence was unaffected.

Conclusions: At the high pressure and temperature conditions relevant to metal-silicate segregation in the Earth's mantle, Mo valence remains relatively constant at about Mo^{3+}, somewhat lower than the Mo^{4+} assumed for core formation models. No Mo^{6+} occurs below IW-1 for a wide range of pressure and temperature conditions, consistent with the interpretations of previous authors [1,3,5,6]. Below IW-1, the contribution of low valence Mo increases, but the mixed average valence never decreases below Mo^{2+}, even at IW-5. It is not clear whether the nugget effect is contributing to the low valence, even though metal is not visible, but metal contributions will be further investigated.

References: [1] Holzheid A. et al. (1994) *Geochim. Cosmochi. Acta*, 58, 1975-1981. [2] Righter K. et al. (1998) *Geochim. Cosmochi. Acta*, 62, 2167-2177. [3] Righter K. and Drake M. J. (1999) *Earth Planet. Sci. Let.*, 171, 383-399. [4] Righter K. (2002) *Icarus*, 158, 1-13. [5] Righter K. et al. (2010) *EPSL*, 291, 1-9. [6] Acuff K. M. (2008) *LPSC XXXIX* 2329. [7] O'Neill H. St.C. and Eggins S. M. (2002) *Chem. Geo.*, 186,151-181. [8] Danielson L.R. et al. (2010) *LPSC XLI* 1946 [9] Berthet et al. (2009) *GCA* 73, 6402-6420 [10] Danielson L. R. et al. (2008) *LPSC XXXIX* 2075. [11] Sutton et al. (2002) *Reviews on Mineralogy & Geochemistry; Appl of Synchrotron Rad in Low-T Geochem & Environ Sci*, Fenter, Rivers, Sturchio, Sutton, eds., *Min. Soc. Amer.*, 429 - 483. [12] Farges F. et al. (2006) *Can. Mineral.*, 44, 731-753. [13] Farges F. et al. (2006) *Can. Mineral.*, 44, 755-773.

Acknowledgements: Portions of this work were performed at GeoSoilEnviroCARS (Sector 13), Advanced Photon Source (APS), Argonne National Laboratory. GeoSoilEnviroCARS is supported by the National Science Foundation - Earth Sciences (EAR-0622171) and Department of Energy - Geosciences (DE-FG02-94ER14466). Use of the Advanced Photon Source was supported by the U. S. Department of Energy, Office of Science, Office of Basic Energy Sciences, under Contract No. DE-AC02-06CH11357.

Table 1. Experiments analyzed from this and previous studies. Silicate composition is indicated above experiment labels. High pressure experiments [3,5,6] were metal-silicate partitioning studies, while controlled atmosphere experiments had no metal added to the starting composition. Mo content of some high pressure experiments is estimated based on previous results [8] to be <10 ppm.

	T deg C	Pressure	Δ IW	Mo, ppm	valence
hawaiite[#]					
66	1300	10 kbar	-0.72	11.78	3.7
67	1300	10 kbar	-0.84	0.49	2.7
68	1300	10 kbar	-0.72	0.91	2.7
74	1300	10 kbar	-0.7	3.74	2.7
76	1300	10 kbar	-0.69	4.79	2.7
80	1300	10 kbar	-0.66	8.23	2.8
83	1300	10 kbar	-0.63	4.61	4.0
87	1300	10 kbar	-0.68	0.11	2.9
basalt[#]					
cow IW	1300	1 bar	0	<10	2.4
cow IW-2	1300	1 bar	-2	<10	1.6
cow1	1500	10 kbar	-1.44	2.9	4.3
cow3	1600	10 kbar	-1.48	4.2	4.3
cow8	1700	10 kbar	-1.45	4.9	4.5
cow20	1800	10 kbar	-1.44	6	4.2
cow D1	1600	10 kbar	-5	<10	2.2
cow c2	1600	10 kbar	-4	<10	2.7
cow b1	1600	10 kbar	-2.8	<10	2.6
BJJB 126	2100	16 GPa	-1	<10	3.3
BJJB 130	2200	24 GPa	-5	<10	2.9
BJJB 134	2100	25 GPa	-1	<10	3.5
ankaramite					
ankIW	1300	1 bar	0	500	5.5
ankIW1	1300	1 bar	1	500	5.9
ankIW2	1300	1 bar	2	500	5.7
ankIW-1	1300	1 bar	-1	500	5.1
ankIW-2	1300	1 bar	-2	500	4.2
andesite[#]					
KR-D	1190	1 bar	11.5	0.13 wt%	6